Journal of Hazardous Materials 209–210 (2012) 218–225

Contents lists available at SciVerse ScienceDirect

Journal of Hazardous Materials

journal homepage: www.elsevier.com/locate/jhazmat

Adsorption isotherms and kinetics studies of malachite green on chitin hydrogels

Hu Tang, Weijie Zhou, Lina Zhang*

Department of Chemistry, Wuhan University, Wuhan 430072, China

ARTICLE INFO

Article history:
Received 14 July 2011
Received in revised form
29 December 2011
Accepted 4 January 2012
Available online 11 January 2012

Keywords:
Chitin hydrogel
Malachite green
Adsorption

ABSTRACT

A chitin hydrogel with concentration 3 wt% (CG3) was successfully prepared from chitin solution dissolved in 8 wt% NaOH/4 wt% urea aqueous system at low temperature by crosslinking with 5 wt% epichlorohydrin. The experimental results revealed that CG3 exhibited high efficiency to remove dye (malachite green) from aqueous solution, as a result of their microporous structure, large surface area and affinity on the dye. The equilibrium process was described well by the Langmuir isotherm model, showing a monolayer adsorption. From kinetic experiments, the adsorption process followed the pseudo-second-order kinetic model, indicating that the overall rate of dye uptake could be controlled by external mass transfer at the beginning of adsorption, while intraparticle diffusion controlled the overall rate of adsorption at a later stage. The activation energy calculated from Arrhenius equation and the result of SEM and FTIR indicated that the adsorption of malachite green on the CG3 was physical process. This work provided an attractive adsorbent for removing of the hazardous materials from wastewater.

1. Introduction

Environmental problems have become a global concern because of their impact on public health. Nearly 25% of the diseases facing humans today occur because long-term exposure to environmental pollution, including air, soil, and water pollution [1]. Dyeing effluent is one of the largest contributors to textile field and such wastewater has a seriously destructive impact on the human health [2]. Dyes, such as malachite green (MG), have been found to be useful in many industrial applications, it is highly effective against important protozoal and fungal infections, and aquaculture industries have been using malachite green extensively as a topical treatment by bath or flush methods. In addition, it is also used as a food coloring agent, food additive, and a medical disinfectant and anthelminthic as well as a dye in silk, wool, jute, and leather cotton, paper and acrylic industries [3]. To prevent dyes discharge and contamination, the removal of dyes from aqueous environment via various methods such as advance oxidation [4], photocatalysis [5], adsorption [6], membrane filtration [7], and coagulation [8], have been reported. Among these methods, the adsorption technique is especially attractive because of its high efficiency, simplicity of design, and ease of operation [9]. Many adsorbents have been tested on the possibility to lower dye concentrations from aqueous solutions, such as activate carbon, clay, peat, chitin, silica, and others [10,11].

Chitin is an abundant biomacromolecule, existing in different crustaceans, mollusks, algae, insects, fungi, and yeasts on earth [12,13]. Because of the linear (1,4)-β-N-acetyl glycosaminoglycan structure with two hydroxyl groups and an acetamide group, chitin is highly crystalline with strong hydrogen bonding, and is very difficult to dissolve in common solvents [14]. This biopolymer has been extensively investigated as adsorbents for the removal of hazardous materials from wastewater, and its efficient adsorption potential can be attributed to high hydrophilicity and high chemical reactivity due to large number of functional groups [15]. Recently, we demonstrated that NaOH/urea aqueous solution can dissolve chitin via a freezing/thawing method to obtain chitin solution [16–18]. Moreover, pure chitin hydrogel has been successfully prepared [14], showing excellent mechanical properties and biocompatibility. Thus we are very interested in preparing chitin hydrogel for wastewater treatment. In this work, we attempted to prepare novel adsorbing material – chitin hydrogel through dissolving it in 8 wt% NaOH/4 wt% urea aqueous solution and then to cross-link it by epichlorohydrin (ECH) [19,20]. This study reported, for the first time, the feasibility of chitin as low-cost alternative adsorbent for malachite green color removal from aqueous solution. The effects of the initial MG concentration, reaction temperature and pH on MG adsorption onto chitin hydrogels were studied. Adsorption kinetics, isotherms and thermodynamic parameters were also evaluated and discussed.

* Corresponding author. Tel.: +86 27 87219274; fax: +86 27 68762005.
E-mail addresses: lnzhang@public.wh.hb.cn, linazhangwhu@gmail.com (L. Zhang).

0304-3894/$ – see front matter.
doi:10.1016/j.jhazmat.2012.01.010

2. Experimental

2.1. Materials

Chitin was supplied by Zhejiang Golden-Shell Biochemical Co., Ltd., China. The weight-average molecular weight (M_w) of chitin, was measured by dynamic light scattering (DLS, ALV/CGS-8F, ALV, Germany) in 5% LiCl/DMAc (w/w), were 5.0×10^5 [14]. Its degree of acetylation (DA) was calculated to be 95% from the nitrogen content according to $DA = 1 - [(W_C/W_N - 5.14)/1.72] \times 100\%$, where W_C/W_N is the ratio of carbon to nitrogen. Epichlorohydrin (ECH) (1.18 g/mL) was of analytical-grade, and was used without further purification. All of the chemical agents including H_2SO_4, NaOH, HCl, $Pb(NO_3)_2$, $HgCl_2$, $CuSO_4{\cdot}5H_2O$ were of analytical grade and were purchased from commercial sources in China.

2.2. Preparation of chitin hydrogels

To prepare the chitin solutions, 3 g chitin was immersed in 97 g of 8 wt% NaOH/4 wt% urea/88 wt% water and stored under refrigeration (−20 °C) for 8 h, then resultant frozen solid was thawed and stirred extensively at room temperature. The freezing/thawing cycle was repeated three times to obtain a transparent chitin solution, with polymer concentration of 3%. Subsequently, 0.05 mL ECH as cross-linker was added to 1 g of the chitin solution, stirred at room temperature for 0.5 h to obtain a homogeneous solution, and then kept at room temperature for 1 h to transform into hydrogels. Finally, the hydrogels were immersed in distilled water for 3 days to remove NaOH and urea. The chitin hydrogel samples were coded as CG3, according to the chitin concentration of 3 wt%.

2.3. Characterization

FTIR of the CG3 sample before and after dye adsorption was recorded with a spectrum one FTIR Spectrometer (model 1600, PerkinElmer Co., USA). Pressed pellets were prepared by grinding the powder specimens with KBr in an agate mortar.

The surface and fracture section of the CG3 sample were observed by using a scanning electron microscope (SEM, Hitachi, S-570, Japan). CG3 was frozen directly in liquid nitrogen, immediately snapped, and then freeze-dried under vacuum. The cross-section of the CG3 was coated with carbon and gold, to be observed and photographed.

2.4. Adsorption studies

The efficiency of the removal of MG from aqueous solutions by CG3 was studied recording to the adsorption isotherms, kinetic experiments and effects of pH. Adsorption isotherms were measured by using batch equilibrium method. Adsorption experiments were carried out in 250 mL beakers containing 40 mL with different MG concentrations for 48 h. Concentrations of MG in aqueous solution were from 0.2 to 1.4 mmol L^{-1}. To each beaker, the same amount of CG3 (weight = 10 g) was added, and then all the beakers were sealed to minimize evaporation.

The concentration of MG in the aqueous solutions was determined with UV spectrophotometer. The amount of MG adsorbed on CG3 was calculated by the following equation [21]:

$$q_e = \frac{(c_0 - c_e)V}{W} \quad (1)$$

where q_e is the amount of MG adsorbed onto the unit amount of the CG3 (mmol g^{-1}), c_0 is the initial concentration of MG (mmol L^{-1}), c_e is the final or equilibrium concentration of MG (mmol L^{-1}), V is the volume of MG solution (L) and W is the weight of CG3 (g).

Kinetic experiments were performed by using different beakers containing around 10 g of CG3 in 40 mL of the dye solution (0.8 mmol L^{-1}). At desired time intervals, the remaining amount of dye in the aqueous solution was then determined by UV spectrophotometery.

To study the effect of pH on the dye removal by CG3, the experiments were carried out at different pH ranging from 3 to 10. Tested samples were prepared by adding 10 g of CG3 to 40 mL of a dye solution (0.8 mmol L^{-1}), pH was adjusted by using NaOH or HCl, and the pH was regularly measured. After 48 h, the resultant solutions were analyzed. In order to obtain thermodynamic parameters, the same procedures were also performed at the solution temperatures of 283, 293 and 303 K.

3. Results and discussion

3.1. Effect of pH on adsorption of MG onto CG3

The influence of pH on the MG adsorption onto CG3 was studied while the MG concentration and adsorption time were fixed at 0.8 mmol L^{-1} and 20 h, respectively. Fig. 1 shows the effect of pH on equilibrium adsorption of the MG dye on the CG3. The results revealed that the physical adsorption occurred between pH 3 and 7, and the equilibrium adsorption of the MG dye on the CG3 achieved to maximum at pH 7. At pH less than 3 there was very small amount of removal of dye by the adsorbent. It can be explained by the fact that at this acidic pH, H^+ may compete with dye ions for the adsorption sites of adsorbent, formed MGH^{+2} species [21–23], thereby inhibiting the adsorption of dye. Above the pH value of 8, the adsorbed amount of MG was slightly higher that at pH 7, and remained almost constant. However, this was as a result of the interaction between cationic MG and the hydroxyl ions in the aqueous solution [24], leading to the weakening of the MG color due to the producing white precipitate of MG [25,26].

3.2. Effect of contact time on adsorption of MG onto CG3

Fig. 2 shows the dependence of the q_e value of MG for adsorption onto CG3 versus the contact time at different initial concentrations. The q_e increased rapidly in the initial stages with an increase of the contact time, and then gradually increased until equilibrium. In addition, the curve of the contact time is smooth and continuous leading to saturation, indicating the possible monolayer coverage of MG on the surface of the sorbent [27].

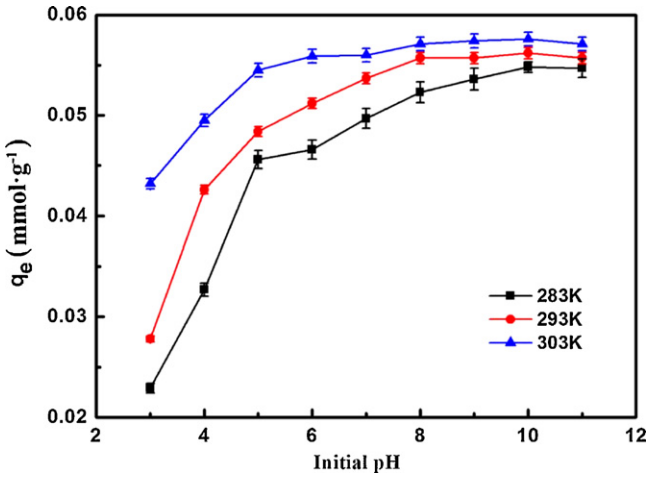

Fig. 1. The effect of pH on the MG adsorption into CG3 at 283, 293 and 303 K.

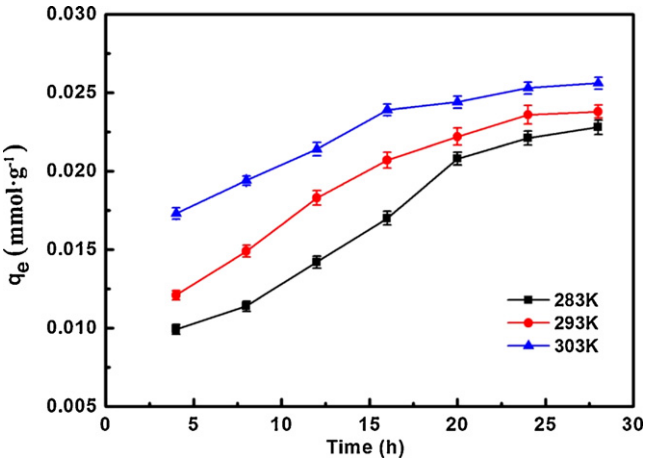

Fig. 2. The effect of contact time on the MG adsorption into CG3 at 283, 293 and 303 K.

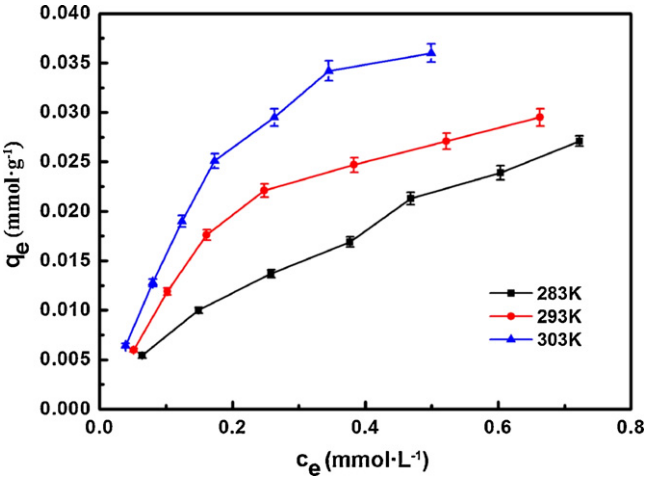

Fig. 3. Adsorption isotherms of MG on CG3 at 283, 293 and 303 K.

3.3. Adsorption isotherms

Adsorption isotherm expressed the relationship between the mass of dye adsorbed at constant temperature per unit mass of the sorbent and the liquid phase dye concentration. To quantify the sorption capacity of sorbent for MG sorption, two-parameter equations namely Langmuir and Freundlich have been adopted in this work. Fig. 3 shows the MG sorption isotherms at 283, 293 and 303 K, respectively. The results indicated that the q_e values increased slightly with an increase of dye concentration. For example, the q_e values of CG3 increased from 0.006 to 0.036 mmol g^{-1}, whereas the dye concentration increased from 0.2 to 1.4 mmol L^{-1} at 303 K. The amount of MG adsorbed on CG3 was raised by increasing temperature.

The Langmuir isotherm model is valid for monolayer adsorption onto a surface with a finite number of identical sites. It is represented in the following form [28]:

$$\frac{1}{q_e} = \frac{1}{q_{\max}} + \frac{1}{q_{\max} b}\frac{1}{c_e} \quad (2)$$

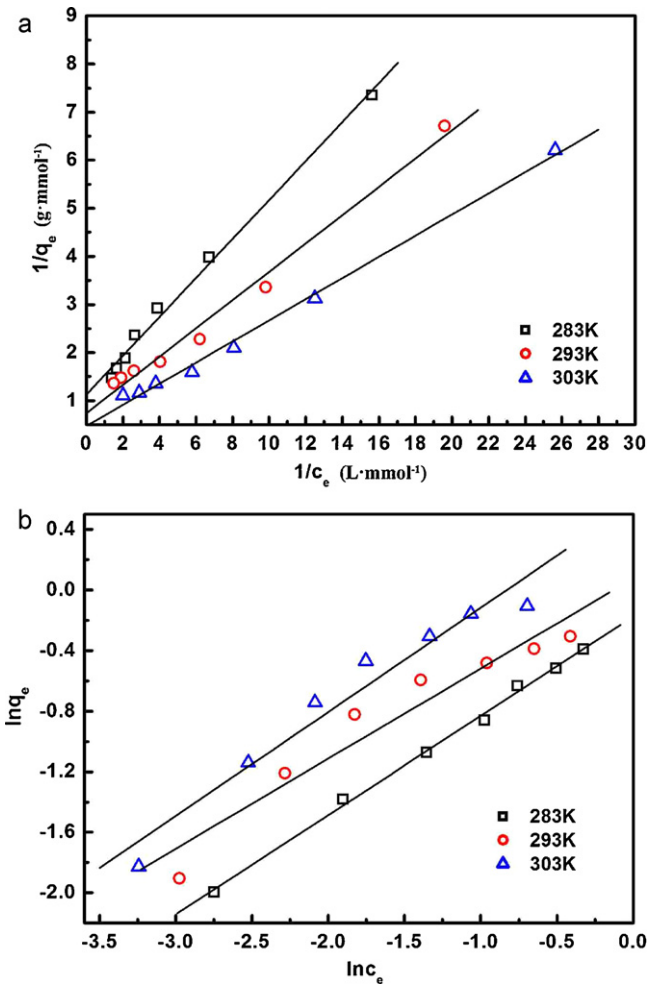

Fig. 4. Langmuir isotherms (a) and Freundlich isotherms (b) for MG adsorption on CG3 at different temperatures.

where $q_{\max}$ is the maximum adsorption at monolayer coverage (mmol g^{-1}) and b is the Langmuir adsorption equilibrium constant (L mmol^{-1}), reflecting the energy of adsorption.

The Freundlich isotherm model is an empirical equation assuming that the adsorption process takes place on heterogeneous surfaces. It is represented in the following form [28]:

$$\ln\ q_e = \frac{1}{n}\ln c_e + \ln K_F \quad (3)$$

K_F and $1/n$ are the Freundlich characteristic constants, indicating adsorption capacity and adsorption intensity, respectively.

Fig. 4a shows Langmuir isotherms for MG adsorption. The calculated results of Langmuir isothermal adsorption parameters for the adsorption of MG are summarized in Table 1. The $q_{\max}$ values gave approximate evaluation of the adsorption amount of MG on the CG3. It was revealed that the CG3 adsorbent exhibited high adsorption capacity for the MG organic dye in the aqueous solution.

Fig. 4b shows Freundlich (Fig. 5b) isotherms for MG adsorption. The Freundlich constant $(1/n)$ is related to the sorption intensity

Table 1
Langmuir and Freundlich parameters for MG adsorption into CG3.

	Langmuir parameters			Freundlich parameters		
	$q_{\max}$ (mmol g^{-1})	b (L mmol^{-1})	R^2	$1/n$	K_F (mmol g^{-1})	R^2
283 K	0.058	2.77	0.9965	0.66	0.018	0.9984
293 K	0.081	2.5	0.9936	0.59	0.010	0.9648
303 K	0.092	2.15	0.9973	0.69	0.017	0.9755

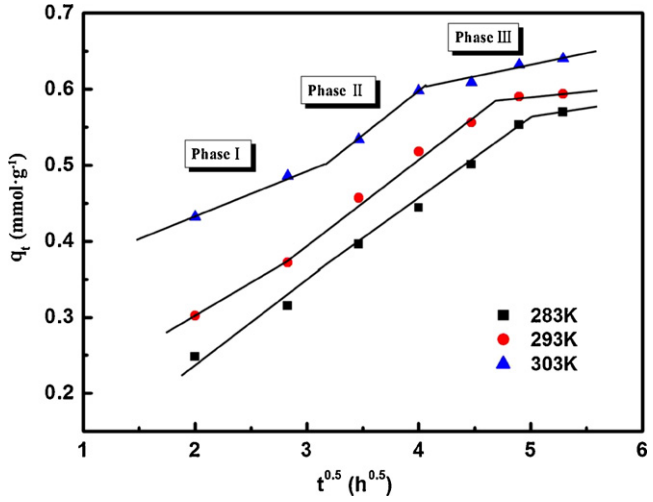

Fig. 5. Intra-particle diffusion plots for MG adsorption at different temperatures.

of the sorbent. When, $0.1 < 1/n \leq 0.5$, adsorption is wonderful; $0.5 < 1/n \leq 1$, it is easy to adsorb; $1/n > 1$, there is difficult to adsorb [29]. As shown in Table 1, the $1/n$ was 0.66 at 283 K; 0.59 at 293 K; 0.69 at 303 K. The $1/n$ value of MG lied in the range from 0.5 to 0.7 indicating that MG could be easily to be adsorbed on the CG3. The MG adsorptive behavior on CG3 was better fitted by Langmuir equation under the concentration range studied (correlation coefficient, $R^2 > 0.99$). It indicated that MG adsorbed on CG3 as a monolayer adsorption.

3.4. Adsorption kinetics

The research of adsorption kinetics describes the dye uptake rate and evidently this rate controls the residence time of adsorbent uptake at the solid-solution interface [30]. In our findings, several kinetic models including the pseudo first order equation, pseudo second order equation, intra-particle diffusion model and Bangham model were applied to find out adsorption mechanism.

3.4.1. The pseudo-first order equation and the pseudo-second order equation

The process of dye removal from aqueous phase by a certain adsorbent may be represented by pseudo-first-order kinetics or pseudo-second-order kinetics [31,32].

The pseudo-first-order kinetic equation is expressed in the form:

$$\frac{1}{q_t} = \left(\frac{k_1}{q_1}\right)\left(\frac{1}{t}\right) + \frac{1}{q_1} \tag{4}$$

The pseudo-second-order kinetic equation is expressed in the form:

$$\frac{t}{q_t} = \frac{1}{k_2 q_2^2} + \left(\frac{1}{q_2}\right) t \tag{5}$$

where q_t is the amount of MG adsorbed (mmol g^{-1}) on CG3 at various time t, q_1 the maximum adsorption capacity (mmol g^{-1}) for the pseudo first order adsorption, k_1 the pseudo-first-order rate constant for the adsorption process (h^{-1}), q_2 the maximum adsorption capacity (mmol g^{-1}) for the pseudo-second-order adsorption, k_2 the rate constant of pseudo-second-order for the adsorption (g mmol^{-1} h^{-1}). The k_1, k_2, q_1, q_2 and correlation coefficients R_1^2 and R_2^2 of MG under different conditions were calculated from these plots, and are given in Table 2. The values of adsorption capacity, q_2, calculated from the pseudo-second-order kinetic equation are more close to the values observed experimentally, q_e than q_1. In addition, the coefficients (R_1^2) for pseudo-first-order kinetic model are between 0.9815 and 0.9934 and the correlation coefficients (R_2^2) for pseudo-second-order kinetic model are between 0.9993 and 0.9997. From these results, the adsorption system obeys the pseudo-second-order kinetic model [33].

Table 2
Kinetic parameters for MG adsorption into CG3 at different temperatures.

	283 K	293 K	303 K
The pseudo-first-order			
k_1 (h^{-1})	208	26.02	5.04
q_1 (mmol g^{-1})	0.045	0.011	0.074
R_1^2	0.9934	0.9815	0.9875
The pseudo-second-order			
k_2 (g mmol^{-1} h^{-1})	0.11	0.19	0.57
q_2 (mmol g^{-1})	0.021	0.025	0.027
R_2^2	0.9996	0.9993	0.9997
Intraparticle diffusion			
k_p (mmol g^{-1} h$^{-0.5}$)	0.103	0.095	0.067
C (mmol g^{-1})	0.012	0.03	0.036
R_p^2	0.9871	0.9889	0.9848

3.4.2. Intra-particle diffusion model

Adsorption is a multi-step process involving transport of solute molecules from the aqueous phase to the surface of the solid particles of adsorbent, and then diffusion of the solute molecules into the interior of the pores, which is likely to be a slow process, and is therefore, rate determining. The intra-particle diffusion parameter, k_p (mmol g^{-1} h$^{-0.5}$) is defined by equation

$$q_t = k_p t^{0.5} + C \tag{6}$$

where k_p is the intra-particle diffusion rate constant (mmol g^{-1} h$^{-0.5}$) and C is a constant. According to this model q_t versus $t^{0.5}$ should be linear if intra-particle diffusion is involved in the adsorption process [34]. The plot of q_t against $t^{0.5}$ may present a multi-linearity correlation, which indicates that three steps occur during adsorption process. The first sharper portion is transport of dye molecules from the bulk solution to the adsorbent external surface by diffusion through the boundary layer (film diffusion). The second portion is the diffusion of the dye molecules from the external surface into the pores of the adsorbent. The third portion is the final equilibrium stage, where the dye molecules were adsorbed on the active sites on the internal surface of the pores and the intra-particle diffusion starts to slow down due to the solute concentration getting lower and lower in solution [35,36].

In Table 2, the correlation coefficients (R_p^2) for the intra-particle diffusion model were between 0.9848 and 0.9871, indicating that the intra-particle diffusion was not the only rate controlling step, other process could control the rate of adsorption. From Eq. (6), if pore diffusion is the rate limiting step, then a plot of q_t against $t^{0.5}$ must give a straight line with a slope that equals k_p and the intercept value c represents the resistance to mass transfer in the external liquid film.

Fig. 5 shows the pore diffusion plot of MG adsorption on CG3. Clearly, the plots are multilinear, containing at least three linear segments. The linear portions of curves did not pass through the origin, suggesting that pore diffusion is not the step controlling the overall rate of mass transfer at beginning of adsorption. The boundary layer effect may control the rate of mass transfer in the time period of the first linear segment, this conclusion could be corroborated by the analysis of data from Boyd's model [37–39].

The model of Boyd is expressed as:

$$F = 1 - \frac{6}{\pi^2}\exp(-Bt) \tag{7}$$

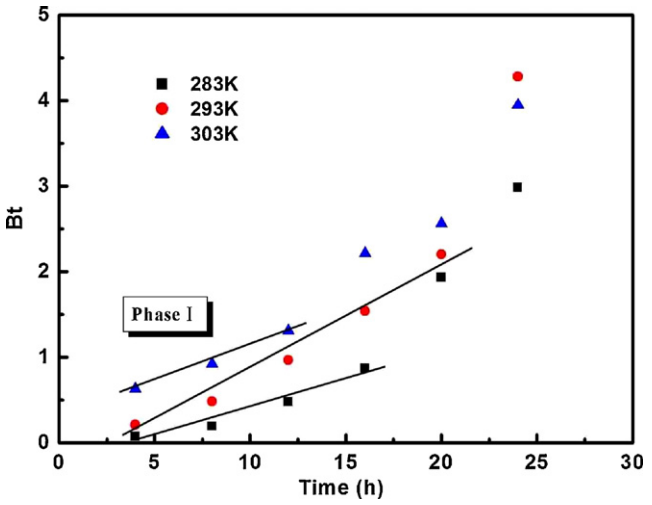

Fig. 6. Boyd plots for MG adsorption at different temperatures.

where F is the fractional attainment of equilibrium, at different times, t, and Bt is a function of F

$$F = \frac{q_t}{q_e} \tag{8}$$

where q_t and q_e are the dye uptake (mmol g^{-1}) at time t and at equilibrium, respectively.

Eq. (7) can be rearranged to

$$Bt = -0.4977 - \ln(1 - F) \tag{9}$$

Fig. 6 shows the values of Bt were calculated from Eq. (9) and plotted against time t. The linearity of this plot can provide available information to distinguish intra-particle diffusion and boundary layer effect (film diffusion) rates of adsorption. If a plot of Bt versus t is a straight line passing through the origin, then adsorption will fit layer effect. The plots are linear only in the initial period of adsorption and do not pass through the origin, indicating that external mass transfer is the rate limiting process in the beginning of adsorption and then is the intra-particle diffusion.

3.5. Thermodynamic parameters of adsorption

Both enthalpy and entropy are the key factors to be considered in any process design [40]. It is essential to clarify the change of thermodynamic parameters to evaluate the feasibility and endothermic nature of the adsorption process, such as standard free energy (ΔG°), enthalpy change (ΔH°), and entropy change (ΔS°). Gibbs energy change, ΔG° are estimated by applying thermodynamic equation [41].

$$\Delta G^\circ = -RT \ln K_d \tag{10}$$

The van't Hoff equation can be used to calculate the values of ΔH° and ΔS°;

$$\ln K_d = \frac{\Delta S^\circ}{R} - \frac{\Delta H^\circ}{RT} \tag{11}$$

where K_d is the equilibrium constant at temperature T, R gas constant (8.314 J mol^{-1} K^{-1}), T absolute temperature (K). The Gibbs free energy indicates a spontaneous and favorable adsorption process. As shown in Table 3, the values of ΔG° for adsorption of MG were −1.89, −2.52 and −3.3 kJ mol^{-1} at 283, 293 and 303 K. The ΔG° value is negative at all studied temperatures, inferring that the adsorption of MG on CG3 would follow a spontaneous and favorable trend. The ΔG° value decreased with an increase in the temperature from 283 K to 303 K. This revealed an increase in adsorption of MG with increasing temperature [42]. In addition, more energetically favorable adsorption occurred 303 K [43]. ΔH° and ΔS° were calculated from the slope and intercept of van't Hoff plots of ln K_d versus $1/T$. From Fig. 7, the ΔH° and ΔS° values were 20.99 kJ mol^{-1} and 80.1 J mol^{-1} K^{-1}, respectively. The positive value of ΔH° suggested the endothermic nature of the adsorption process. The positive value of ΔS° suggested good affinity of MG towards the CG3 and increased randomness at the solid-solution interface [44].

Table 3
Thermodynamic parameters for adsorption of MG into CG3.

Temperature (K)	ΔH° (KJ mol^{-1})	ΔS° (J mol^{-1} K^{-1})	ΔG° (kJ mol^{-1})
283 K	20.99	80.1	−1.89
293 K			−2.52
303 K			−3.3

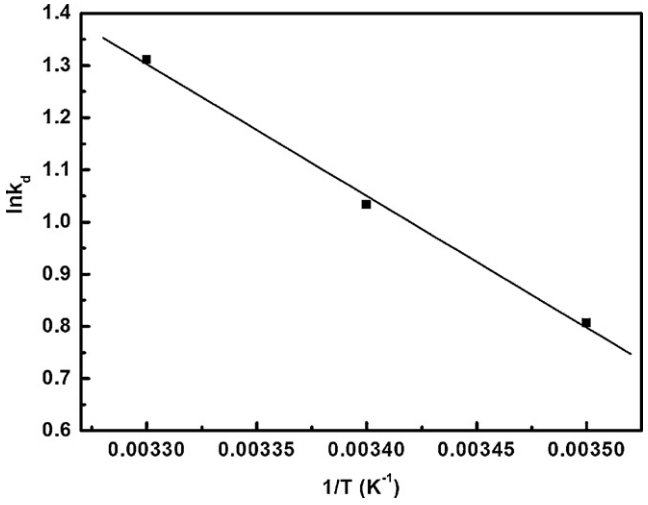

Fig. 7. van't Hoff plot for MG adsorption on CG3.

Arrhenius equation is expressed as below

$$\ln\ k_2 = \ln A - \frac{E_a}{RT} \tag{12}$$

where k_2 is the rate constant of pseudo-second order adsorption (g mg^{-1} h^{-1}), A the Arrhenius factor, R gas constant (8.314 J mol^{-1} K^{-1}), T absolute temperature (K). The activation energy (E_a) can be calculated from Arrhenius equation, which is used to determine the type of adsorption. As shown in Fig. 8, the E_a for MG adsorption on CG3 was 37.18 kJ mol^{-1}. Generally, low

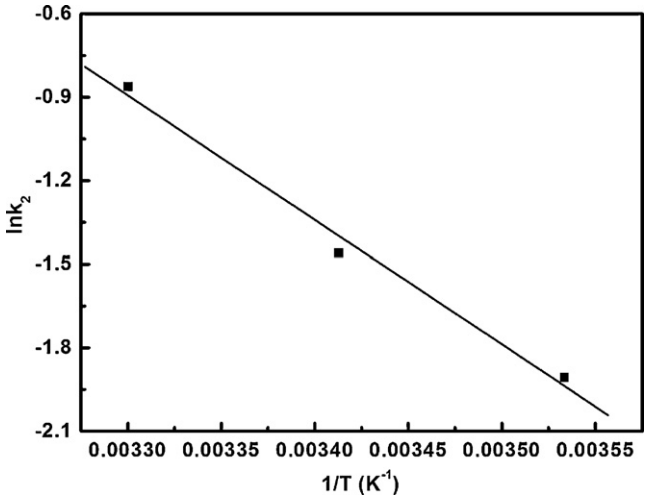

Fig. 8. The Arrhenius plot for MG adsorption on CG3.

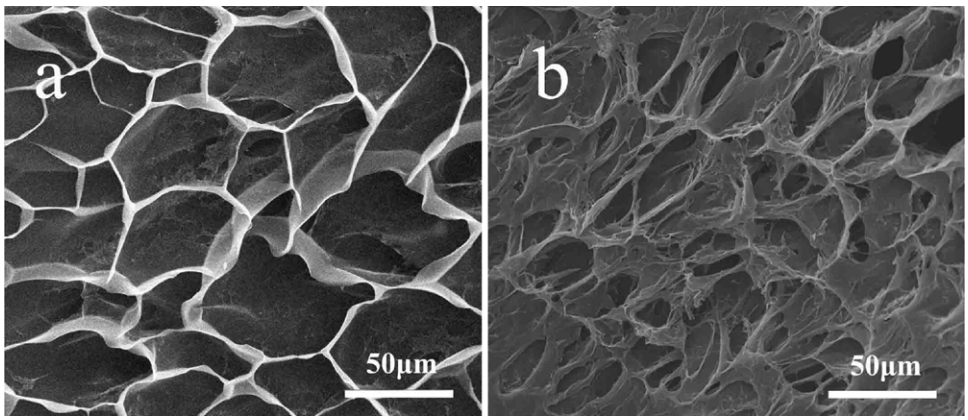

Fig. 9. SEM photographs of the CG3 (cross-section) before (a) and after (b) adsorption of MG.

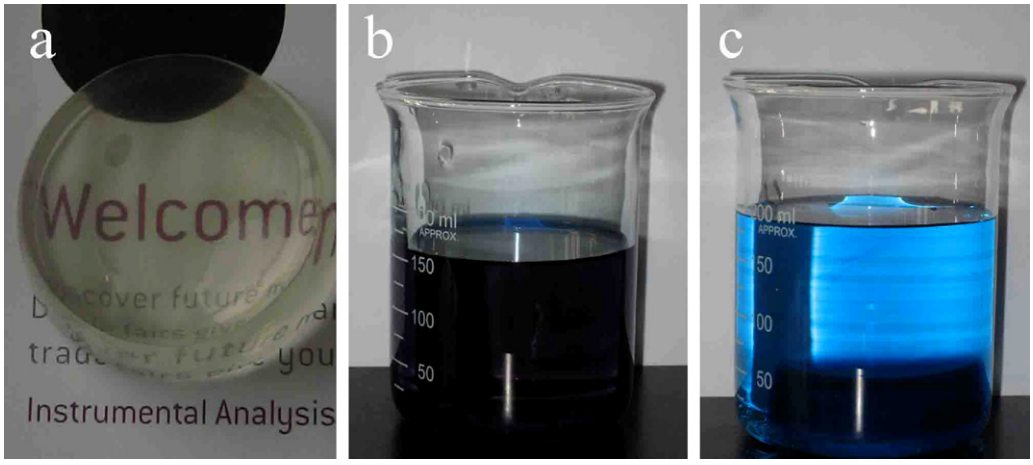

Fig. 10. Photograph of the CG3 (a), the adsorption process before (b) and after adsorption of MG (c) at pH 7.

activation energies (5–40 kJ mol^{-1}) are characteristic of physical adsorption, while high ones (40–800 kJ mol^{-1}) suggest chemisorptions [45]. Therefore, the physical adsorption mechanism occurred here, and there was an energy barrier in the adsorption process [3,46].

3.6. Adsorption interaction between molecules

SEM is one of the most widely used surface and cross-section diagnostic tools. Fig. 9 shows SEM photographs of the CG3 (cross-section) before (a) and after (b) adsorption of MG. The SEM results displayed well-defined, interconnected, three-dimensional porous structures with significant micropores with mean size of 20 μm. Noticeably, these pores had regular and very thin wall before adsorption of MG, suggesting the orderly aggregate of chitin chains. The chitin having semi-stiff molecular chain played an important role in enhancing the strength of hydrogel. Namely, the relative stiff chitin chains were contributed to support the pore wall to encage many MG, whereas their —OH and —NHCOCH$_3$ groups acted as adsorbent of MG. The pore size of CG3 after adsorption (Fig. 9b) was obviously smaller than before (Fig. 9a). It was indicated that the malachite green was filled in the pore via an intermolecular interaction. It was not hard to imagine that the porous chitin matrix was very suitable for the sorption of malachite green. There was a tight binding between the dye and the adsorbent [3,24].

The pictures of the adsorption process of the dyes are shown in Fig. 10. The CG3 was very transparent (Fig. 10a), after 16 h, the wastewater changed to be almost colorless (Fig. 10b and c). The dyes MG could be adsorbed by the CG3 within 4 h, supporting the strong interaction between chitin and MG. The results demonstrated that the CG3 could purify water effectively to remove the MG.

FTIR spectrum is a useful tool to identify hydrogen bonding. The FTIR spectra (500–4000 cm^{-1}) of the CG3 before and after adsorption are shown in Fig. 11. Usually, the major peak for

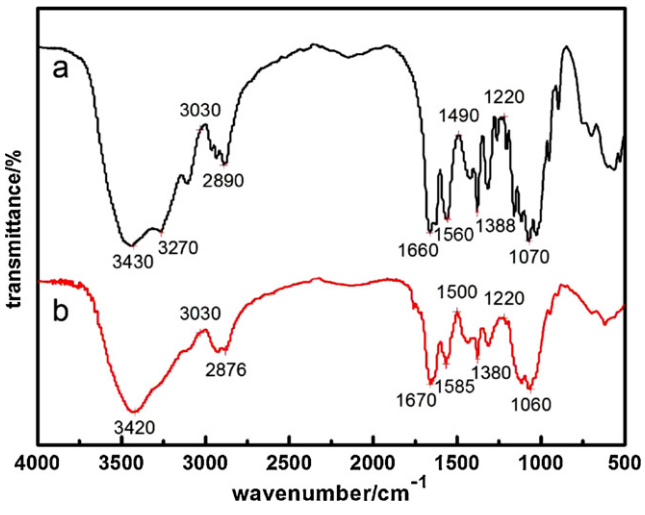

Fig. 11. FTIR spectra of CG3 before (a) and after (b) adsorption of MG.

chitin are located at around 3430 cm^{-1} for O—H stretching vibration, 3260 cm^{-1} for N—H stretching vibration, 1660 cm^{-1} (amide I), 1623 and 1557 cm^{-1} (amide II) correspond to N—H bending vibrations [47]. Interestingly, MG-loaded CG3 exhibited characteristic changes of the hydroxyl groups and the acetyl groups, which shifted from 3430, 1660 (amide I) and 1560 cm^{-1} (amide II) before malachite green adsorption to 3420, 1670 and 1585 cm^{-1} after adsorption. The small band at 3258 cm^{-1} was due to stretching vibration of N—H groups, which disappeared exactly in the spectrum of Chit-MG. These changes could be owing to strong interaction of MG with OH— groups and acetyl groups. The bands at 2890 cm^{-1} and 1388 cm^{-1} shown in Fig. 11 are assigned to the C—H stretching and bending vibration of polymer backbone, respectively. There was significant decrease for the bands in the spectrum of malachite green, and the bands were shifted from 2890, 1388 to 2876, 1380 cm^{-1}. This can be considered as the evident for the interaction between chitin and MG.

4. Conclusion

The CG3 absorbent was successfully prepared in 8 wt% NaOH/4 wt% urea aqueous solution via a freezing/thawing method to dissolve chitin, and then by crosslinking with 5 wt% epichlorohydrin. CG3 exhibited microporous structure, large surface area and affinity on malachite green, leading to the high uptake capacity of dye. The relative stiff chitin chains were contributed to support the pore wall to encage many MG, whereas their —OH and —$NHCOCH_3$ groups acted as adsorbent of MG, leading to the attractive adsorption for removing of MG wastewater. Moreover, the adsorption of MG was dependent on initial concentration, reaction temperature and pH. The MG adsorption capacity increased with the increase of pH in the range of 3–8, where physical adsorption occurred. The adsorption equilibrium could be well described by Langmuir adsorption isotherms, namely monolayer adsorption on a homogenous surface. The activation energy calculated from Arrhenius equation and the result of SEM and FTIR indicated that the adsorption of malachite green on the CG3 was further confirmed to be physical process. Thermodynamic results indicated that process was spontaneous and endothermic.

Acknowledgments

This work was supported by National Basic Research Program of China (973 Program, 2010CB732203), and the National Natural Science Foundation of China (20474048 and 20874079).

References

[1] L. Zhou, C. Gao, W. Xu, Magnetic dendritic materials for highly efficient adsorption of dyes and drugs, ACS Appl. Mater. Interfaces 2 (2010) 1483–1491.
[2] R. Blackburn, Natural polysaccharides and their interactions with dye molecules: applications in effluent treatment, Environ. Sci. Technol. 38 (2004) 4905–4909.
[3] Z. Bekçi, C. Özveri, Y. Seki, K. Yurdakoç, Sorption of malachite green on chitosan bead, J. Hazard. Mater. 154 (2008) 254–261.
[4] B. Shi, G. Li, D. Wang, C. Feng, H. Tang, Removal of direct dyes by coagulation: the performance of preformed polymeric aluminum species, J. Hazard. Mater. 143 (2007) 567–574.
[5] J. Lee, S. Choi, R. Thiruvenkatacharib, W. Shim, H. Moon, Submerged microfiltration membrane coupled with alum coagulation/powdered activated carbon adsorption for complete decolorization of reactive dyes, Water Res. 40 (2006) 435–444.
[6] D. Mahanta, G. Madras, S. Radhakrishnan, S. Patil, Adsorption and desorption kinetics of anionic dyes on doped polyaniline, J. Phys. Chem. B 113 (2009) 2293–2299.
[7] D. Mahanta, G. Madras, S. Radhakrishnan, S. Patil, Adsorption of sulfonated dyes by polyaniline emeraldine salt and its kinetics, J. Phys. Chem. B 112 (2008) 10153–10157.
[8] W. Chen, W. Lu, Y. Yao, M. Xu, Highly efficient decomposition of organic dyes by aqueous-fiber phase transfer and in situ catalytic oxidation using fiber-supported cobalt phthalocyanine, Environ. Sci. Technol. 41 (2007) 6240–6245.
[9] Y. Wong, Y. Szeto, W. Cheung, G. McKay, Equilibrium studies for acid dye adsorption onto chitosan, Langmuir 19 (2003) 7888–7894.
[10] J. Fernández, J. Kiwi, C. Lizama, J. Freer, J. Baeza, H. Mansilla, Factorial experimental design of orange II photocatalytic discolouration, J. Photochem. Photobiol. A 151 (2002) 213–219.
[11] S. Tahir, N. Rauf, Removal of a cationic dye from aqueous solutions by adsorption onto bentonite clay, Chemosphere 63 (2006) 1842–1848.
[12] S. Ifuku, S. Morooka, M. Morimoto, H. Saimoto, Acetylation of chitin nanofibers and their transparent nanocomposite films, Biomacromolecules 11 (2010) 1326–1330.
[13] L. Zhang, H. Tang, C. Chang, China Patent ZL, 201010201892.3 (2010).
[14] C. Chang, S. Chen, L. Zhang, Novel hydrogels prepared via direct dissolution of chitin at low temperature: structure and biocompatibility, J. Mater. Chem. 21 (2011) 3865–3871.
[15] G. Crini, Recent developments in polysaccharide-based materials used as adsorbents in wastewater treatment, Prog. Polym. Sci. 30 (2005) 38–70.
[16] J. Cai, L. Zhang, S. Liu, Y. Liu, X. Xu, X. Chen, B. Chu, X. Guo, J. Xu, H. Cheng, C. Han, S. Kuga, Dynamic self-assembly induced rapid dissolution of cellulose at low temperatures, Macromolecules 41 (2008) 9345–9351.
[17] C. Chang, B. Duan, L. Zhang, Fabrication and characterization of novel macroporous cellulose–alginate hydrogels, Polymer 50 (2009) 5467–5473.
[18] C. Chang, J. Peng, L. Zhang, D. Pang, Strongly fluorescent hydrogels with quantum dots embedded in cellulose matrices, J. Mater. Chem. 19 (2009) 7771–7776.
[19] P. Sikorski, R. Hori, M. Wada, Revisit of α-chitin crystal structure using high resolution X-ray diffraction data, Biomacromolecules 10 (2009) 1100–1105.
[20] S. Ifuku, M. Nogi, K. Abe, M. Yoshioka, M. Morimoto, H. Saimoto, H. Yano, Preparation of chitin nanofibers with a uniform width as α-chitin from crab shells, Biomacromolecules 10 (2009) 1584–1588.
[21] B. Samiey, A. Toosi, Adsorption of malachite green on silica gel: effects of NaCl, pH and 2-propanol, J. Hazard. Mater. 184 (2010) 739–745.
[22] B. Samiey, M. Dargahi, Kinetics of brilliant green fading in the presence of TX-100, DTAB and SDS, React. Kinet. Mech. Catal. 101 (2010) 25–39.
[23] B. Noroozi, G. Sorial, H. Bahrami, M. Arami, Equilibrium and kinetic adsorption study of a cationic dye by a natural adsorbent-Silkworm pupa, J. Hazard. Mater. B 139 (2007) 167–174.
[24] B. Samiey, A. Raoof Toosi, Kinetics of malachite green fading in the presence of TX-100, DTAB and SDS, Bull. Korean Chem. Soc. 30 (2009) 2051–2056.
[25] B. Samiey, A. Toosi, Kinetics of malachite green fading in alcohol–water binary mixtures, Int. J. Chem. Kinet. 42 (2010) 508–518.
[26] E. Baumann, Colorimetric determination of low pH with malachite green, Talanta 42 (1995) 457–462.
[27] A. Rodríguez, G. Ovejero, M. Mestanza, J. García, Removal of dyes from wastewaters by adsorption on sepiolite and pansil, Ind. Eng. Chem. Res. 49 (2010) 3207–3216.
[28] G. Bayramoglu, A. Denizli, S. Bektas, M. Arica, Entrapment of lentinus sajorcaju into ca-alginate gel beads for removal of Cd(II) ions from aqueous solution: preparation and biosorption kinetics analysis, Microchem. J. 72 (2002) 63–67.
[29] B. Samiey, M. Dargahi, Kinetics and thermodynamics of adsorption of Congo red on cellulose, Central Eur. J. Chem. 8 (2010) 906–912.
[30] M. Sulak, E. Demirbas, M. Kobya, Removal of astrazon yellow 7GL from aqueous solutions by adsorption onto wheat bran, Bioresour. Technol. 98 (2007) 2590–2598.
[31] S. Mohan, N. Rao, J. Kartikeyan, Adsorptive removal of direct AZO dye from aqueous phase onto coal based sorbents: a kinetic and mechanistic study, J. Hazard. Mater. B 90 (2002) 189–204.
[32] Y. Ho, G. McKay, Sorption of dye from aqueous solution by peat, Chem. Eng. J. 70 (1998) 115–124.
[33] A. Özcan, A. Özcan, Adsorption of acid dyes from aqueous solution onto acid-activated bentonite, J. Colloid Interface Sci. 276 (2004) 39–46.
[34] I. Kiran, T. Akar, A. Özcan, A. Özcan, S. Tunali, Biosorption kinetics and isotherm studies of acid red 57 by dried cephalosporium aphidicola cells from aqueous solutions, Biochem. Eng. J. 31 (2006) 197–203.
[35] Q. Sun, L. Yang, The adsorption of basic dyes from aqueous solution on modified peat-resin particle, Water Res. 37 (2003) 1535–1544.
[36] B. Hameed, M. El-Khaiary, Kinetics and equilibrium studies of malachite green adsorption on rice straw-derived char, J. Hazard. Mater. 153 (2008) 701–708.
[37] B. Koumanova, P. Peeva, S. Allen, Variation of intraparticle diffusion parameter during adsorption of *p*-chlorophenol onto activated carbon made from apricot stones, J. Chem. Technol. Biotechnol. 78 (2003) 582–587.
[38] A. Özcan, E. Öncu, A. Özcan, Adsorption of acid blue 193 from aqueous solutions onto DEDMA-sepiolite, J. Hazard. Mater. B 129 (2006) 244–252.
[39] G. Boyd, A. Adamson, L. Meyers, The exchange adsorption of ions from aqueous solution by organic zeolites. II. Kinetics, J. Am. Chem. Soc. 69 (1947) 2836–2848.
[40] C. Ijagbemi, M. Baek, D. Kim, Montmorillonite surface properties and sorption characteristics for heavy metal removal from aqueous solutions, J. Hazard. Mater. 166 (2009) 538–546.
[41] L. Juang, C. Wang, C. Lee, Adsorption of basic dyes onto MCM-41, Chemosphere 64 (2006) 1920–1928.
[42] S. Khattria, M. Singh, Removal of malachite green from dye wastewater using neem sawdust by adsorption, J. Hazard. Mater. 167 (2009) 1089–1094.
[43] Z. Aksu, E. Kabasakal, Batch adsorption of 2,4-dichlorophenoxy-acetic acid (2-4-D) from aqueous solution by granular activated carbon, Sep. Purif. Technol. 35 (2004) 223–240.

[44] X. Sun, S. Wang, X. Liu, W. Gong, N. Bao, B. Gao, H. Zhang, Biosorption of malachite green from aqueous solutions onto aerobic granules: kinetic and equilibrium studies, Bioresour. Technol. 99 (2008) 3475–3483.
[45] M. Dogan, M. Alkan, O. Demirbas, Y. Ozdemir, C. Ozmetin, Adsorption kinetics of maxilon blue GRL onto sepiolite from aqueous solutions, Chem. Eng. J. 124 (2006) 89–101.
[46] M. Baek, C. Ijagbemi, S.O.D. Kim, Removal of malachite green from aqueous solution using degreased coffee bean, J. Hazard. Mater. 176 (2010) 820–828.
[47] J. Dong, Y. Ozaki, FTIR and FT-Raman studies of partially miscible poly(methyl methacrylate)/poly(4-vinylphenol) blends in solid states, Macromolecules 30 (1997) 286–292.